Nanoscale

PAPER

View Article Online
View Journal | View Issue

Cite this: *Nanoscale*, 2014, **6**, 8032

Structural characterisation of a layered double hydroxide nanosheet†

Nicholas P. Funnell,[a] Qiang Wang,[ab] Leigh Connor,[c] Matthew G. Tucker,[cd] Dermot O'Hare*[a] and Andrew L. Goodwin*[a]

Received 7th March 2014
Accepted 12th May 2014

DOI: 10.1039/c4nr01265h

www.rsc.org/nanoscale

We report the atomic-scale structure of a Zn_2Al–borate layered double hydroxide (LDH) nanosheet, as determined by reverse Monte Carlo (RMC) modelling of X-ray total scattering data. This study involves the extension of the RMC method to enable structural refinement of two-dimensional nanomaterials. The refined LDH models show the intra-layer geometry in this highly-exfoliated phase to be consistent with that observed in crystalline analogues, with the reciprocal-space scattering data suggesting a disordered arrangement of the Zn^{2+} and Al^{3+} cations within the nanosheet. The approach we develop is generalisable and so offers a method of characterising the structures of arbitrary nanosheet phases, including systems that support complex forms of disorder within the nanosheets themselves.

The extreme anisotropy of single-layer nanomaterials gives rise to a range of novel physical and chemical properties of intense current interest in the development of advanced functional materials.[1] On a fundamental level, ultrathin materials such as graphene, molybdenum disulfide and boron nitride have been shown to exhibit high electron mobilities, quantum Hall effects, extreme thermal conductivities, magnetic resonant modes and superconductivity.[2–9] But nanosheet phases are also of practical importance: the recent development of inorganic graphene analogues offering the combination of high-energy-density capacitance and deformability required for the growing market of flexible displays and devices is one representative example;[10] their application within composite materials to enhance permeability, flame retardancy, and thermal stability another.[11–16]

A recurring challenge within this field is the difficult problem of characterising the atomic-scale structures of single-layer phases, as is needed to direct material optimisation: conventional crystallographic techniques fail because they rely on the presence of three-dimensional structural periodicity. Total scattering (or pair distribution function, PDF) measurements are a promising crystallographic alternative finding increasing traction within the nanomaterials community.[17] The appeal is that the PDF is well-defined—and measurable—even in the absence of long-range periodicity.[18–20] Yet instances where PDF methods have been applied to ultrathin materials remain scarce because the most accessible tools of PDF analysis also operate within the context of a three-dimensional unit cell.[21,22] What is urgently needed within the field is an atomistic method of refining PDF data that is sufficiently adaptable to model the complex structures adopted by nanomaterials.

In this study, we extend the reverse Monte Carlo (RMC) approach[23] to enable atomistic refinement of ultrathin phases, and apply this methodology to the structure determination of a Zn/Al double hydroxide nanosheet. Layered double hydroxides (LDHs) are a well-established and versatile family of inorganic materials with applications in CO_2 capture,[24] drug delivery,[25,26] fire retardation,[27,28] and catalysis.[29,30] An important recent advance in their chemistry has been preparation of highly-dispersed, unmodified, delaminated nanosheet LDHs *via* the so-called aqueous miscible organic solvent treatment (AMOST) technique.[11] AMO-LDHs are dispersible in non-polar hydrocarbons and possess BET surface areas in excess of 450 $m^2\ g^{-1}$; moreover they are anticipated to outperform 'bulk' LDH phases for use as sorbents, catalyst precursors and nano-additives.[11,26,31] While bulk LDHs are known to adopt a brucite-like crystal structure in which positively-charged layers of hydroxide-bridged metal cations are separated by weakly-coordinated water molecules and interlayer anions [Fig. 1(a)],[32] the structure of nanosheet LDHs is extremely difficult to determine reliably. When measured using a conventional laboratory X-ray diffractometer, their diffraction patterns contain only two peaks over the 2θ angular range 5–65°, with both peaks suffering from extreme Warren-type anisotropy [Fig. 1(b)].[33] The determination of metal coordination geometries or nanosheet structure by Rietveld refinement is simply not possible from such data;

[a]*Inorganic Chemistry Laboratory, Department of Chemistry, University of Oxford, South Parks Road, Oxford, OX1 3QR, UK. E-mail: dermot.ohare@chem.ox.ac.uk; andrew.goodwin@chem.ox.ac.uk*

[b]*College of Environmental Science and Engineering, Beijing Forestry University, 35 Qinghua East Road, Haidan District, Beijing 100083, China*

[c]*Diamond Light Source, Harwell Science and Innovation Campus, Fermi Avenue, Didcot, OX11 0QX, UK*

[d]*ISIS Facility, Rutherford Appleton Laboratory, Harwell Science and Innovation Campus, Didcot, OX11 0QX, UK*

† Electronic supplementary information (ESI) available. See DOI: 10.1039/c4nr01265h

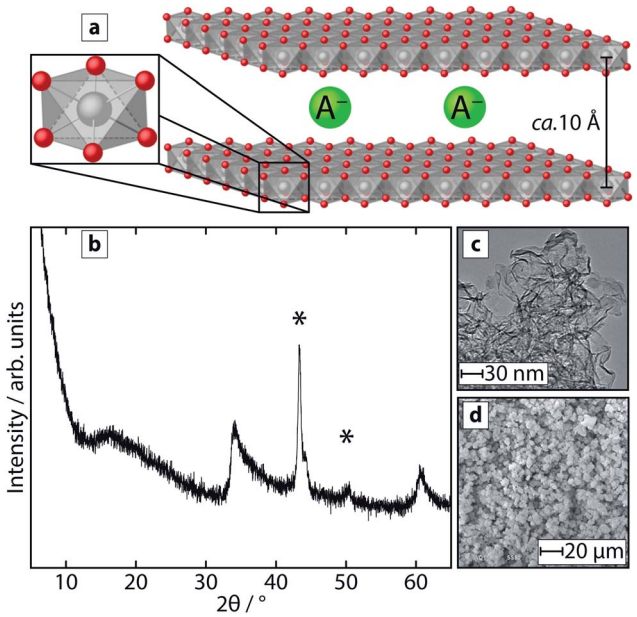

Fig. 1 (a) Schematic of a typical crystalline LDH structure; edge-linked metal octahedra form sheets, spaced by interlayer anions (A^-; here, predominantly borate). (b) PXRD pattern of the AMOST-prepared Zn_2Al–borate LDH. In the crystalline parent compound, (00*l*) peaks are evident in PXRD patterns typically between *ca.* 10–25°. Asterisks denote scattering from the sample container. TEM and SEM images of the sample are shown in (c and d). Panels (b–d) are adapted from ref. 11.

indeed this is a good example of the general problem of structural characterisation of nanosheet phases.

PDF methods have been applied previously to bulk LDHs and in these cases have given useful insight into aspects such as thermal decomposition,[34] iodine intercalation,[35] and the existence and nature of stacking faults.[36] However—to the best of our knowledge—the technique has not yet been applied to exfoliated LDH nanosheets. Nor has it been possible to explore the extent of cation ordering in nanosheet LDHs, in spite of the intense interest in (and controversy over) using charge distribution to tailor LDH functionality.[35–38] So our motivation for using RMC methods to characterise the atomic-scale structure of an LDH nanosheet is threefold. First, we sought to establish whether exfoliation has any substantial effect on metal coordination geometries or other aspects of the structural chemistry of the LDH layers. Second, we have used this case study as a means of extending the RMC refinement approach[23,39] to the challenging problem of determining nanosheet structures. Third, we exploit the ability of RMC refinements to explore variable cation ordering motifs to establish whether there is any experimental sensitivity to Zn/Al ordering within the LDH nanosheet at the heart of our study. Our results indicate that the local metal coordination geometries within the nanosheet are comparable to those found in analogous bulk crystalline phases, and also that the distribution of Zn^{2+} and Al^{3+} ions is not strongly ordered.

An exfoliated sample of Zn_2Al–borate LDH was prepared *via* the AMOST method as described in ref. 11, using acetone as the dispersing solvent. The X-ray powder diffraction pattern of this sample, collected using a typical in-house X-ray diffractometer, is that shown in Fig. 1(b). The absence of (00*l*) reflections from this pattern is characteristic of a highly-exfoliated nanosheet phase; the two observed peaks near $2\theta = 35°$ and 62° correspond instead to the intra-layer (110) and (200) reflections. Transmission and scanning electron microscopy images also reflect the single-layer nature of the sample [Fig. 1(c) and (d)]. Using the I12 beamline at the Diamond Light Source and a Thales Pixium area detector, we measured X-ray total scattering data (λ = 0.14577 Å) for magnitudes of the scattering vector **Q** between 0.5 and 33 $Å^{-1}$. The diffraction images were integrated over this angular range using the FIT2D software,[40–42] yielding an uncorrected powder-averaged diffraction pattern. These data were processed using GUDRUNX,[43,44] in order to correct for background scattering, Compton scattering, multiple scattering and beam attenuation by the sample container, giving the normalised total scattering function $F(Q)$ and the corresponding PDF (noting we have used the $D(r)$ normalisation as described by eqn (26) in ref. 45 and a Q_{max} value of 17 $Å^{-1}$; see ESI† for further details). Our data are shown in Fig. 2(a) and (b); we emphasise the contrast in information density relative to the X-ray diffraction pattern of Fig. 1(b).

In order to derive a structural model from these total scattering data, we have developed an atomistic approach based on the reverse Monte Carlo (RMC) method. This approach, which is

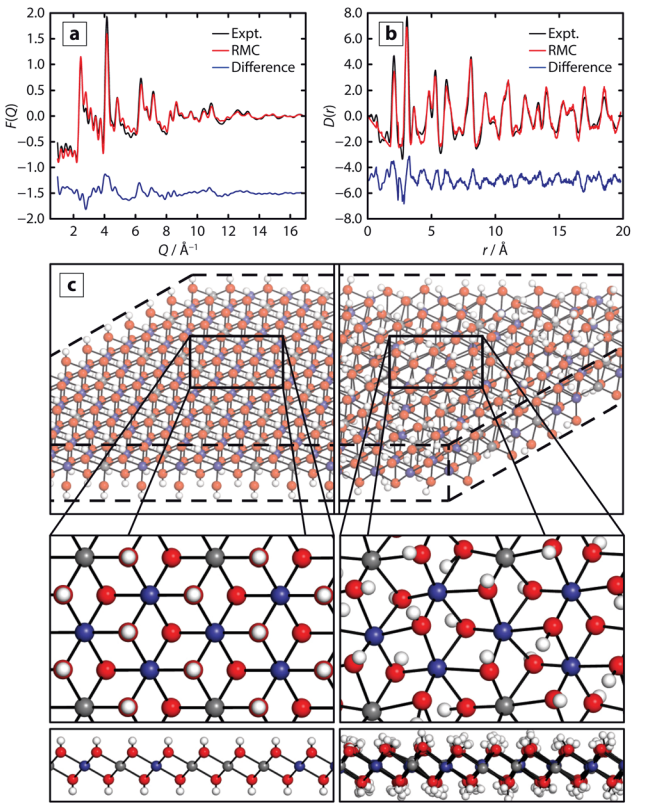

Fig. 2 RMC-refined total scattering pattern (a) and PDF (b). (c) Shows representative cross-sections of the LDH nanosheet model prior to (left) and post-RMC refinement (right). Al atoms are shown in grey, Zn in blue, O in red and H in white.

outlined below (full details are given as ESI†) contrasts the alternative 'real-space Rietveld' method[46] applied elsewhere to structure refinement of related nanostructured materials. Our motivation for developing an atomistic approach lies in the additional configurational versatility offered: the exploration of Zn/Al ordering tendency is one such application. While RMC methods are well established for three-dimensional materials—crystalline and disordered alike—the modelling of lower-dimensional nanostructures is an ongoing challenge.[18] The primary difficulty lies in treating appropriately the existence of periodic boundary conditions that might be considered to apply only in some directions.

In general terms the approach we have taken is as follows. Our RMC configuration contains a single nanosheet which is oriented parallel to one of the faces of the simulation box and which extends across the entire box in the two in-plane directions. The remainder of the RMC box is empty, with the box size in the direction perpendicular to the nanosheet chosen to be larger than either of the in-plane directions. In this way, the maximum distance up to which pair correlations are calculated is determined only by the in-plane dimensions of the nanosheet. The PDF calculated from such a box, $D_{\mathrm{RMC}}(r)$, is related to the 'real' $D(r)$ after two corrections are made: (i) the difference in number density between the simulation box (which is mostly empty) and the real material is taken into account, and (ii) the (unstructured) pair correlations between atoms within the model nanosheet and atoms in the surrounding material are included. Taken together, one obtains

$$D(r) = D_{\mathrm{RMC}}(r) + 4\pi r\rho\delta(r)\sum_{i,j} c_i c_j f_i f_j \left[\frac{\rho_{\mathrm{RMC}}}{\rho} - \frac{d}{2r}\right], \qquad (1)$$

where ρ_{RMC} and ρ are the simulation and real number densities, respectively, the c_i and f_i the concentrations and scattering factors of the atomic species i, and d the width of the nanosheet. The parameter $\delta(r) = 0$ for $r \leq d/2$ and 1 for $r > d/2$ (*i.e.* the correction is always positive). The total scattering function $F(Q)$ can be corrected in a similar way (see ESI†).

Using this approach we proceeded to carry out a RMC refinement of the atomic-scale structure of Zn_2Al–borate LDH against the X-ray total scattering data collected as described above. Our hexagonal configurations (dimensions 45.81 Å × 45.81 Å × 100 Å) contained a total of 75 Al atoms, 150 Zn atoms, 450 O atoms, and 450 H atoms. Borate anions were explicitly omitted from our model on the basis that there is no strong case for assuming coherent ordering of these units relative either to the nanosheet or to one other. The likely effect of this decision is that one does not expect quantitative fitting for the low-r region of the PDF where B–O and O–(B–)O correlations will contribute in a coherent sense to the experimental PDF. The box size we have chosen corresponds to a 15 × 15 supercell of the layer unit cell shown in Fig. 1(a), the dimensions of which were determined from the position of the (110) reflection in the diffraction pattern. Atoms were placed according to the known LDH layer structure with the Zn/Al distribution chosen randomly; the nearest-neighbour connectivity was fixed accordingly. Soft constraints on Zn–O, Al–O and O–H bond lengths and (Zn/Al)–O–H, O–(Zn/Al)–O and (Zn/Al)–O–(Zn/Al) angles were applied (see ESI† for details). Since the H atom contribution to the X-ray scattering function is negligible, we expected the H atom positions in the final model to reflect these constraints more closely than any real signature of H atom correlations actually contained within the data. Following the standard RMC approach, atoms were chosen at random and moved by small random amounts until the fit to data (both $F(Q)$ and $D(r)$) converged satisfactorily. The fits obtained are shown in Fig. 2(a) and (b) and a comparison between starting and refined structures is given in Fig. 2(c).

As anticipated, the quality of the fits obtained is noticeably inferior to the typical results for RMC refinements of crystalline materials.[47–50] The most significant discrepancies are for the lowest-r region of the $D(r)$ function where (i) intra-borate correlations are not accounted for by the model, and (ii) the nanosheet correction in eqn (1) switches from zero to finite value. Further uncertainties in the true sample density ρ (or indeed what this means for a nanosheet sample), layer thickness d, anion composition and water content mean that quantitative fitting is very much more difficult in this case. Nevertheless the general features of the PDF are certainly well described by the refined RMC configurations, and even the Warren peak asymmetry in the $F(Q)$ function is appropriately modelled. The RMC configuration can be collapsed onto a single 'unit cell' (noting that this cell is periodic only in two directions), the corresponding *layer* group symmetry being $P\bar{3}m1$ in order to determine the effective average coordination geometry of the Zn and Al centres within the nanosheet. This structure, together with the corresponding average bond lengths and angles are illustrated in Fig. 3. We find essentially complete agreement with the coordination geometry found in crystalline Zn/Al LDHs,[35,51] although we do not find any meaningful distinction between Zn and Al environments. We note that the similarity between crystalline and nanosheet structures is consistent with the suggestion elsewhere that because bulk samples can be reconstituted from nanosheets through exposure to water or Na_2CO_3 solutions it is unlikely that exfoliation promotes amorphisation.[11]

Having established the average structure of the LDH nanosheet, we proceeded to address the question of substitutional Zn/Al ordering within individual layers. There is limited

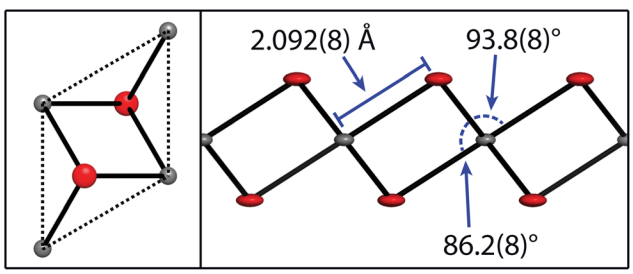

Fig. 3 The LDH nanosheet structure, derived from averaged instantaneous coordinates and their displacements from mean atomic positions. Anisotropic displacement parameters are shown at the 50% probability level. The black dotted lines in the left panel indicate the two-dimensional 'unit cell'. H atoms are omitted owing to the relative insignificance in their spatial distribution. O atoms are shown in red and Zn/Al cations are shown in grey.

evidence that in certain mixed-metal LDHs with $M^{2+}:M^{3+}$ concentrations of 2 : 1 the more highly charged cations avoid sharing hydroxide bridges.[35,37,52] This local rule leads to an ordered structure in which the M^{3+} cations are surrounded only by M^{2+} cations to give a periodic 'honeycomb' motif [Fig. 4(a)]. Using a straightforward Monte Carlo algorithm, we generated a range of RMC configurations with different degrees of Zn/Al ordering; the corresponding order parameter is given by the average number of Al^{3+} 'neighbours' around each Al^{3+} centre, n_{Al}^{Al}. The long-range ordered state of Fig. 4(a) corresponds to the case $n_{Al}^{Al} = 0$, whereas a statistical distribution corresponds to $n_{Al}^{Al} = 2$ [Fig. 4(b)]. We found some evidence of a continuous dependence of the goodness of fit on the value of n_{Al}^{Al} such that the best fit to data is observed for $n_{Al}^{Al} \geq 1$ [Fig. 4(c)]. Consequently our analysis suggests there is no substantive Al/Zn ordering, although it is not clear whether the cation distribution is purely statistical or whether some slight preference for Al/Al avoidance persists. Since we do not find meaningful differences in Zn–O and Al–O distances, the sensitivity we observe must arise from scattering contrast between the Zn and Al centres. It is our experience that the signature of correlated disorder is often stronger in reciprocal space (which emphasises correlations) than in real space.[48,53] Here we find that the quality of the $D(r)$ fit is relatively insensitive to the value of n_{Al}^{Al} [Fig. 4(d)]: in particular, long-range ordered and statistical distributions are only marginally different in terms of their fit to the $D(r)$ function even if they give rise to meaningfully different qualities of fit in reciprocal space.

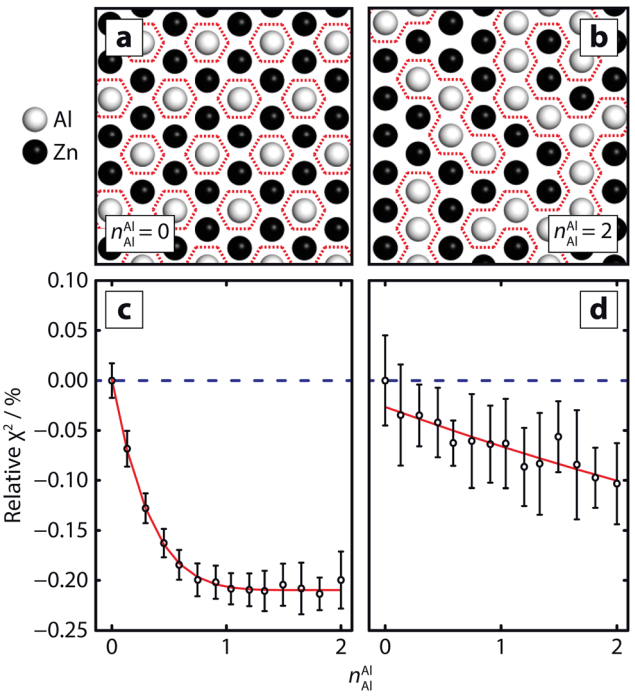

Fig. 4 Cross-sections of ordered (a) and disordered (b) cation arrangements. Oxygen and hydrogen atoms are omitted for clarity. The dotted red lines in (a and b) indicate Al/Zn boundaries. χ^2 values, expressed as the percentage difference from the first data point (blue dotted line), are shown for the $F(Q)$ (c) and $D(r)$ (d) data. The error bars represent the corrected sample standard deviations, each derived from six RMC refinements. The red lines show error-weighted three-parameter polynomial fits of the form $\chi_{rel}^2 = \chi_0^2 + \alpha(n_{Al}^{Al} - n_0)^6$, chosen to capture the particular nonlinearity of the dependency observed in (c).

In some respects there are strong parallels between our study and a recent report in which PDF methods were applied to the problem of determining intermediate-range order in layered cobalt-based nanoparticle catalysts.[22] In terms of the method of analysis employed, the two studies are distinguished by the use of atomistic (RMC) and real-space Rietveld approaches, and also by the incorporation or omission of reciprocal-space scattering data during structure refinement. Atomistic methods offer the flexibility of exploring cation ordering, for example, but real-space Rietveld refinements are advantageous in terms of the level of effort involved. The quality of fit to the experimental PDF reported in ref. 22 would appear better than that we obtain in this study, which is perhaps surprising given that the modelling approaches taken in that study neglect the contribution of intra-anion, inter-anion, and nanoparticle-anion/solvent interactions to the PDF. Here the constraint of fitting in reciprocal space helps emphasise the scattering contribution from the ordered structural component (*i.e.* the nanosheets in our case), and should also ameliorate any spurious effects associated with ignoring differences in the angular dependence of the X-ray form factors for different elements.

In conclusion, X-ray total scattering measurements and RMC refinement of a Zn_2Al–borate LDH nanosheet have been used to determine its atomic-scale structure. We find that the coordination environment of the Zn and Al atoms is similar to that found in crystalline Zn/Al-containing LDHs and that there is no evidence of strong Zn/Al order within the compositional arrangement of the nanosheet, a feature to which the PDF itself appears to be relatively insensitive. Having demonstrated the applicability of RMC methods for studying what is a chemically complex nanostructured material, we anticipate the method presented here will find application in the structural characterisation of other ultrathin nanomaterials, including magnetic nanosheet assemblies, titania-based electrocatalysts and photoluminescent single-layer perovskites.[54–56]

This research was supported by the EPSRC (ALG; grant EP/G004528/2), the ERC (NPF and ALG; project 279705), SCG Chemicals, Bangkok (QW and DOH) and by the Diamond Light Source in the form of access to the I12 beamline.

References

1 H. Duan, N. Yan, R. Yu, C.-R. Chang, G. Zhou, H.-S. Hu, H. Rong, Z. Niu, J. Mao, H. Asakura, T. Tanaka, P. J. Dyson, J. Li and Y. Li, *Nat. Commun.*, 2014, **5**, 3093.
2 K. S. Novoselov, A. K. Geim, S. V. Morozov, D. Jiang, Y. Zhang, S. V. Dubonos, I. V. Grigorieva and A. A. Firsov, *Science*, 2004, **306**, 666–669.
3 K. S. Novoselov, D. Jiang, F. Schedin, T. J. Booth, V. V. Khotkevich, S. V. Morozov and A. K. Geim, *Proc. Natl. Acad. Sci., U. S. A.*, 2005, **102**, 10451–10453.
4 H. He, P. Bourges, Y. Sidis, C. Ulrich, L. P. Regnault, S. Pailhés, N. S. Berzigiarova, N. N. Kolesnikov and B. Keimer, *Science*, 2002, **295**, 1045–1047.

5 K. S. Novoselov, A. K. Geim, S. V. Morozov, D. Jiang, M. I. Katsnelson, I. V. Grigorieva, S. V. Dubonos and A. A. Firsov, *Nature*, 2005, **438**, 197–200.
6 Y. Zhang, Y.-W. Tan, H. L. Stormer and P. Kim, *Nature*, 2005, **438**, 201–204.
7 X. Wang, Y. Ouyang, X. Li, H. Wang, J. Guo and H. Dai, *Phys. Rev. Lett.*, 2008, **100**, 206803.
8 A. K. Geim, *Science*, 2009, **324**, 1530–1534.
9 A. A. Balandin, *Nat. Mater.*, 2011, **10**, 569–581.
10 C. Wu, X. Lu, L. Peng, K. Xu, X. Peng, J. Huang, G. Yu and Y. Xie, *Nat. Commun.*, 2013, **4**, 2431.
11 Q. Wang and D. O'Hare, *Chem. Commun.*, 2013, **49**, 6301–6303.
12 C. Taviot-Guého and F. Leroux, *Struct. Bonding*, 2006, **119**, 121–159.
13 L. Wang, X. He and C. A. Wilkie, *Materials*, 2010, **3**, 4580–4606.
14 Q. Wang, X. Zhang, C. J. Wang, J. Zhu, Z. Guo and D. O'Hare, *J. Mater. Chem.*, 2012, **22**, 19113–19121.
15 F. Leroux and C. Taviot-Guého, *J. Mater. Chem.*, 2005, **15**, 3628–3642.
16 C. Manzi-Nshuti, D. Wang, J. M. Hossenlopp and C. A. Wilkie, *J. Mater. Chem.*, 2008, **18**, 3091–3102.
17 C. A. Young and A. L. Goodwin, *J. Mater. Chem.*, 2011, **21**, 6464–6476.
18 O. Gereben and V. Petkov, *J. Phys.: Condens. Matter*, 2013, **25**, 454211.
19 S. J. L. Billinge, T. Dykhne, P. Juhas, E. Bozin, R. Taylor, A. J. Florence and K. Shankland, *CrystEngComm*, 2010, **12**, 1366–1368.
20 K. Page, T. C. Hood, T. Proffen and R. B. Neder, *J. Appl. Crystallogr.*, 2011, **44**, 327–336.
21 M. Gateshki, S.-J. Hwang, D. H. Park, Y. Ren and V. Petkov, *Chem. Mater.*, 2004, **16**, 5153–5157.
22 C. L. Farrow, D. K. Bediako, Y. Surendranath, D. G. Nocera and S. J. L. Billinge, *J. Am. Chem. Soc.*, 2013, **135**, 6403–6406.
23 M. G. Tucker, D. A. Keen, M. T. Dove, A. L. Goodwin and Q. Hui, *J. Phys.: Condens. Matter*, 2007, **19**, 335218.
24 Q. Wang, Y. Gao, J. Luo, Z. Zhong, A. Borgna, Z. Guo and D. O'Hare, *RSC Adv.*, 2013, **3**, 3414–3420.
25 S. Li, J. Li, C. J. Wang, Q. Wang, M. Z. Cader, J. Lu, D. G. Evans, X. Duan and D. O'Hare, *J. Mater. Chem. B*, 2013, **1**, 61–68.
26 X. Gao, L. Lei, D. O'Hare, J. Xie, P. Gao and T. Chang, *J. Solid State Chem.*, 2013, **203**, 174–180.
27 C. Nyambo and C. A. Wilkie, *Polym. Degrad. Stab.*, 2009, **94**, 506–512.
28 Q. Wang, J. P. Undrell, Y. Gao, G. Cai, J.-C. Buffet, C. A. Wilkie and D. O'Hare, *Macromolecules*, 2013, **46**, 6145–6150.
29 Y. Zhao, M. Wei, J. Lu, Z. L. Wang and Z. Duan, *ACS Nano*, 2009, **3**, 4009–4016.
30 C. G. Silva, Y. Bouizi, V. Fornes and H. Garcia, *J. Am. Chem. Soc.*, 2009, **131**, 13833–13839.
31 Y. Zhao, C. J. Wang, W. Gao, Q. Wang, B. Li, L. Zheng, M. Wei, D. G. Evans, X. Duan and D. O'Hare, *J. Mater. Chem. B*, 2013, **1**, 5988–5994.
32 F. Cavani, F. Trifirò and A. Vaccari, *Catal. Today*, 1991, **11**, 173–301.
33 B. E. Warren, *Phys. Rev.*, 1941, **59**, 693–698.
34 M. C. D. Mourad, M. Mokhtar, M. G. Tucker, E. R. Barney, R. I. Smith, A. O. Alyoubi, S. N. Basahel, M. S. P. Shaffer and N. T. Skipper, *J. Mater. Chem.*, 2011, **21**, 15479–15485.
35 L. Aimoz, C. Taviot-Guého, S. V. Churakov, M. Chukalina, R. Dähn, E. Curti, P. Bordet and M. Vespa, *J. Phys. Chem. C*, 2012, **116**, 5460–5475.
36 A. Faour, C. Mousty, V. Prevot, B. Devouard, A. D. Roy, P. Bordet, E. Elkaim and C. Taviot-Gueho, *J. Phys. Chem. C*, 2012, **116**, 15646–15659.
37 P. J. Sideris, U. G. Nielsen, Z. Gan and C. P. Grey, *Science*, 2008, **321**, 113–117.
38 S. Cadars, G. Layrac, C. Gérardin, M. Deschamps, J. R. Yates, D. Tichit and D. Massiot, *Chem. Mater.*, 2011, **23**, 2821–2831.
39 R. L. McGreevy and L. Pusztai, *Mol. Simul.*, 1988, **1**, 359–367.
40 A. P. Hammersley, S. O. Svensson, M. Hanfland, A. N. Fitch and D. Häusermann, *High Pres. Res.*, 1996, **14**, 235–248.
41 A. P. Hammersley, *FIT2D: An Introduction and Overview, ESRF Internal Report technical report*, 1997.
42 A. P. Hammersley, *FIT2D V9.129 Reference Manual V3.1, ESRF Internal Report*, 1998.
43 S. E. McLain, D. T. Bowron, A. C. Hannon and A. K. Soper, *GUDRUN, a computer program developed for analysis of neutron diffraction data*, Chilton: ISIS Facility, Rutherford Appleton Laboratory.
44 A. K. Soper and E. R. Barney, *J. Appl. Crystallogr.*, 2011, **44**, 714–726.
45 D. A. Keen, *J. Appl. Crystallogr.*, 2001, **34**, 172–177.
46 C. L. Farrow, P. Juhas, J. W. Liu, D. Bryndin, E. S. Božin, J. Bloch, T. Proffen and S. J. L. Billinge, *J. Phys.: Condens. Matter*, 2007, **19**, 335219.
47 E. O. R. Beake, M. T. Dove, A. E. Phillips, D. A. Keen, M. G. Tucker, A. L. Goodwin, T. D. Bennett and A. K. Cheetham, *J. Phys.: Condens. Matter*, 2013, **25**, 396403.
48 E. Dixon, J. Hadermann, S. Ramos, A. L. Goodwin and M. A. Hayward, *J. Am. Chem. Soc.*, 2011, **133**, 18397–18405.
49 D. E. Nanu, M. G. Tucker, W. G. Haije, J. F. Vente and A. J. Böttger, *Acta Mater.*, 2010, **58**, 5502–5510.
50 C. A. Young, E. Dixon, M. G. Tucker, D. A. Keen, M. A. Hayward and A. L. Goodwin, *Z. Kristallogr.*, 2012, **227**, 280–287.
51 M. Bastianini, D. Costenaro, C. Bisio, L. Marchese, U. Costantino, R. Vivani and M. Nocchetti, *Inorg. Chem.*, 2012, **51**, 2560–2568.
52 I. G. Richardson, *Acta Crystallogr.*, 2013, **B69**, 629–633.
53 A. L. Goodwin, M. T. Dove, A. M. Chippindale, S. J. Hibble, A. H. Pohl and A. C. Hannon, *Phys. Rev. B*, 2009, **80**, 054101.
54 S. Ida, C. Ogata, U. Unal, K. Izawa, T. Inoue, O. Altuntasoglu and Y. Matsumoto, *J. Am. Chem. Soc.*, 2007, **129**, 8956–8957.
55 T. Saida, N. Ogiwara, Y. Takasu and W. Sugimoto, *J. Phys. Chem. C*, 2010, **114**, 13390–13396.
56 M. Osada, T. Sasaki, K. Ono, Y. Kotani, S. Ueda and K. Koboyashi, *ACS Nano*, 2011, **5**, 6871–6879.

